

Fabrication of Electrochemical Sensor Based on Molecularly Imprinted Polymer/Zinc Oxide Nanoparticle-Nanocomposite (MIP/ZnO/CPE) for Determination of Cyanazine in Food Samples

Lixin You^{1,2}, Lixia You³, Weihua Qi¹, Nannan Hu¹, Yongjie Sun¹, Fengxian Qin^{1,4,*}, Tiejun Hu^{1,4,*}

¹ Colloge of Life Sciences, Changchun Science and Technology University, Changchun 130600, China

² Jilin Research Center of functional food industry Engineering, Changchun 130600, China

³ Huadian Gongji Township Integrated Service Centre, Jilinhudian 132400, China

⁴ Jilin Deer Industry Engineering Research Center, Changchun 130600, China

*E-mail: zhushikunmama@sina.com and htj1315436996060@sina.com

Received: 27 September 2022 / Accepted: 1 November 2022 / Published: 30 November 2022

The purpose of this research was to create an electrochemical sensor based on a nanocomposite of zinc oxide nanoparticles (ZnO NPs) and molecularly imprinted polymer (MIP) for detecting cyanazine in food samples. To make modified electrodes, ZnO NPs were electrodeposited on the surface of a carbon paste electrode (CPE), and then a MIP layer was electropolymerized on the modified CPE (MIP/ZnO/CPE). Structural studies of modified electrodes revealed the formation of ZnO NPs with hexagonal shape characteristics and a wurtzite-type structure on the CPE surface, and after electropolymerization, polymer nanoparticles were evenly dispersed on the nanostructured surface of ZnO, resulting in the formation of a rough-shaped nanocomposite. Electrochemical measurements using DPV and amperometry revealed a significant increase in MIP/ZnO/CPE electrocatalytic activity and selectivity due to the synergistic effect of ZnO and MIPs. The studies demonstrated a linear response from 0 to 120 μM , and the sensitivity of MIP/ZnO/CPE was determined to be 0.5034 $\mu\text{A}/\mu\text{M}$, with a limit of detection of 5nM. The MIP/ZnO/CPE as a proposed sensing system for cyanazine analysis in real samples prepared from lettuce samples was investigated, and the analytical results showed that the RSD (3.48% to 4.64%) and recovery (99.20% to 99.60%) values were appropriate for valid and accurate practical analyses in food in agricultural wastewater samples.

Keywords: Molecularly Imprinted Polymer; Zinc Oxide Nanoparticle; Nanocomposite; Cyanazine; Electrodeposition; Amperometry

1. INTRODUCTION

Cyanazine ($\text{C}_9\text{H}_{13}\text{ClN}_6$) is the common name for 2-chloro-4-(1-cyano-1-methylethyl-amino)-6-ethylamine-1,3,5-triazine, a triazine herbicide. Cyanazine will cause photosystem dysfunction by

binding to important proteins required for this process [1, 2]. When this critical step in photosynthesis fails, a plant is unable to produce sugars that are necessary for growth and metabolism. As a result, it is used to control annual grasses and broadleaf weeds as a herbicide [3, 4]. It eliminates undesirable vegetation, particularly weeds, grasses, and woody plants. Cyanazine is the most toxic triazine herbicide, and it has been linked to birth defects, mutations, and, eventually, cancer [5]. Depending on the severity of the contact, cyanazine can cause dermatitis [6, 7]. Acute toxicity can also occur when high levels of cyanazine are consumed. Inhaling cyanazine fumes can cause airway irritation [8-10].

Furthermore, because cyanazine quickly washes out of the soil and into the surrounding waters, it is especially harmful to aquatic ecosystems [11, 12]. Cyanazine can cause dermatitis depending on the severity of the contact. When high levels of cyanazine are consumed, acute toxicity can occur. Inhaling cyanazine fumes can irritate the airways [13, 14].

Furthermore, because cyanazine is rapidly washed out of the soil and into the surrounding waters, it is particularly harmful to aquatic ecosystems [15], enzyme-linked immunosorbent assay (ELISA) [16], gas chromatography [17], surface plasmon resonance [18], high-performance liquid chromatography (HPLC) [19], fluorescent [20] and electrochemical sensor [21] for determination cyanazine. However, due to the presence of many interfering substances in food and agricultural wastewater, the selectivity and sensitivity of cyanazine sensors in these studies are relatively limited [22, 23]. More research is thus required to improve the detection performance of herbicide sensors. Electrochemical sensors based on molecularly imprinted polymers (MIPs) have demonstrated commendable precision and selectivity for herbicide determination in real samples containing interferants.[24-26]. These sensors are synthetic materials that are used as recognition elements in sensor design due to their higher thermal stability, reusability, and selectivity compared to biological receptors [27, 28]. Furthermore, MIPs-based electrochemical sensors are simple, quick, and inexpensive. This research focused on the development of an electrochemical sensor based on a nanocomposite of ZnO NPs and MIP for the detection of cyanazine in food samples.

2. MATERIALS AND METHODS

2.1. Synthesis of nanocomposite of ZnO NPs-MIP modified CPE

For preparation of the CPE, 1.4 g graphite powder (99%, Qingdao Furuite Graphite Co., Ltd., China) was added to 0.6 g paraffin liquid (99.9%, Qingdao Fortune Environmental Technology Co., Ltd., China). The mixture was blended in a mortar by hand until a homogeneous paste was obtained. The resultant paste was tightly packed into one end of a PVC tube (3 mm internal diameter) that contained copper wire as electrical contact. The electrode was polished on a clean sheet of butter paper to achieve a smooth surface. Freshly prepared CPE was pretreated in 0.1 M PBS (pH = 5.5) by cycling the potential between 0.4 and 1.4 V vs. Ag/AgCl at a scan rate of 30 mV/s for 15 cycles using a potentiostat/galvanostatic system with a 3-electrode cell, with a platinum plate electrode as a counter-electrode, an Ag/AgCl as reference electrode, and CPE as working electrode [29, 30]. For modification of the CPE surface with ZnO NPs, the CPE was subjected to cyclic potential sweeps, between -1.0 and -0.8 V vs. Ag/AgCl at a scan rate of 30 mV/s for 25 cycles in support electrolyte of 50 mM NaNO₃

($\geq 99.0\%$, Sigma-Aldrich) containing 10 mM ZnCl_2 ($\geq 98\%$, Sigma-Aldrich) [31]. The electrode was immersed in 0.1 PBS (pH = 5.5) containing 5 mM O-Phenylenediamine (99.0%, Sigma-Aldrich) and 1 mM cyanazine (99%, Sigma-Aldrich) for preparation. Poly(o-phenylenediamine) film was electrochemically synthesized for 25 cycles using cyclic potential sweeps between 0.0 and 0.1 V vs. Ag/AgCl at a scan rate of 30 mV/s [32]. To remove the cyanazine template molecules, the MIP modified electrodes were dipped in 0.2 M NaOH (99%, Merck Millipore, Germany) for 5 minutes. As a control, the NIP electrode was also synthesized in the same manner, but without adding cyanazine. Finally, the modified electrodes were stored in a refrigerator at 4 °C.

2.2. Characterizations

Field emission scanning electron microscopy (FESEM) and X-ray diffractometer (XRD) with Cu K radiation (1.5406 Å) at 40 KV and 40 mA were used to analyze the structural and morphological properties of synthesized nanostructures. For electrochemical analyses, amperometry and differential pulse voltammetry (DPV) techniques were used on a potentiostat/galvanostatic system (PARSTAT, mod 2273, Princeton Applied Research, Oak Ridge, USA) in a 0.1 M phosphate buffer solution (PBS) with pH = 4.0 that contained an equal volume ratio of 0.1M NaH_2PO_4 (99%, Sigma-Aldrich) and 0.1M Na_2HPO_4 (99%). 0.1 M HCl (37%, Merck Millipore, Germany) and 0.1 M NaOH were used to adjust the pH of the solutions.

2.3. Analysis of the actual sample

The lettuce was purchased at a local market, washed, and crushed and squeezed with domestic juice extractor. The extracted liquid was filtered through filter paper (Whatman) and centrifuged for 5 minutes at 1000 rpm. The obtained supernatant was used to prepare the real sample as follows: To obtain 1.25 mg/l cyanazine (5.19 μM), 0.250 mg of cyanazine solution was ultrasonically added to 200.0 mL of the resultant supernatant and 200.0 mL of 0.1 M PBS solution which was used as a real sample for amperometric studies. The traditional standard method was also used to analyze the actual sample.

3. RESULTS AND DISCUSSION

3.1. Structural studies of nanostructured modified electrodes

Figure 1 shows FE-SEM micrographs of modified electrodes (ZnO/CPE , $\text{MIP}/\text{ZnO}/\text{CPE}$, and $\text{NIP}/\text{ZnO}/\text{CPE}$). Figure 1a shows a FE-SEM micrograph of ZnO/CPE that shows the formation of nanoparticles and some rods with a hexagonal shape typical of ZnO with a wurtzite-type structure on the surface. The hexagonal cross section of nanoparticles and rods has an average size of 100 nm. The FE-SEM micrographs of $\text{MIP}/\text{ZnO}/\text{CPE}$ and $\text{NIP}/\text{ZnO}/\text{CPE}$ (Figures 1b and 1c) show that after electropolymerization, polymer nanoparticles can be evenly dispersed on the nanostructured surface of ZnO, forming new rough-shaped nanocomposite. The MIP was dipped after the template (cyanazine)

was removed with NaOH. As a result, MIP/ZnO/CPE has a rougher and more porous structure than NIP/ZnO/CPE, and the resulting cavities after template removal are shown in Figure 1b. These cavities can be used for template binding with MIP in electrochemical sensors [33, 34]. Figure 1c shows the surface of NIP, implying no defined pattern or structure on the electrode surface. The results demonstrate that MIPs have more vacant sites and porous surfaces to adsorb template molecules [35-37].

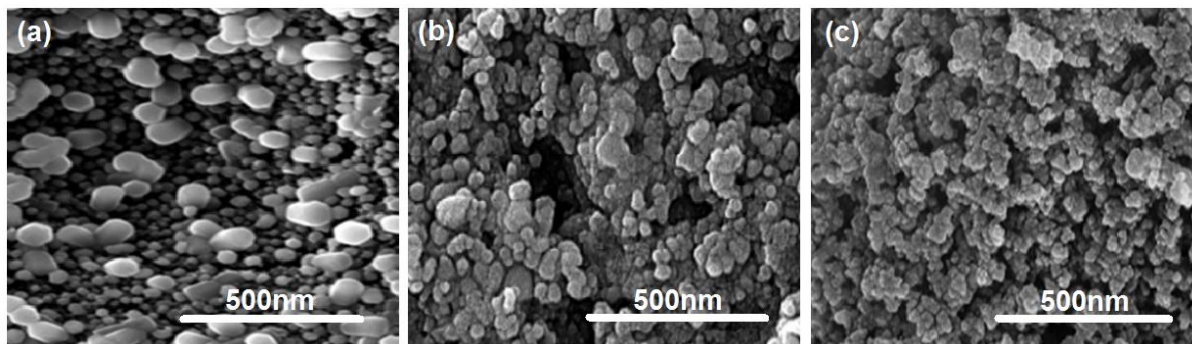


Figure 1. FE-SEM micrographs of modified electrodes (a) ZnO/CPE, (b) MIP/ZnO/CPE and (c) NIP/ZnO/CPE.

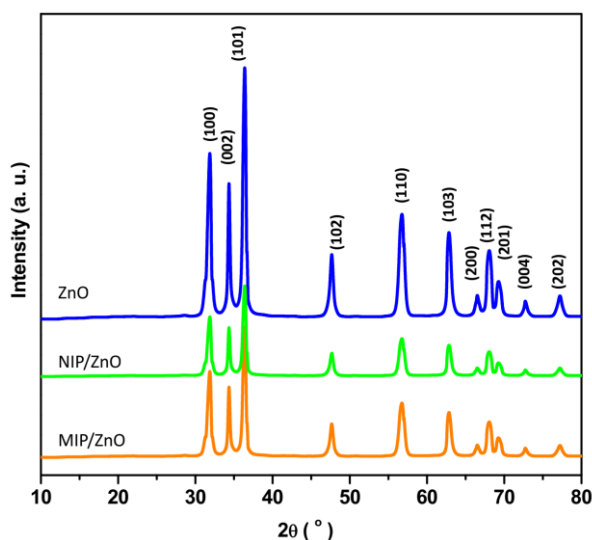


Figure 2. The results of structural characterization of powders of ZnO, MIP/ZnO and NIP/ZnO nanocomposites by XRD.

Figure 2 depicts the structural characterization results of powders of ZnO, MIP/ZnO, and NIP/ZnO nanocomposites. XRD pattern of ZnO depicts characteristic diffraction peak at $2\theta = 31.88^\circ$, 34.32° , 36.29° , 47.56° , 56.59° , 62.8° , 66.49° , 68.02° , 69.20° , 72.6° , 77.03° can be assigned to (100), (002), (101), (102), (110), (103), (200), (112), (201), (004) and (202) Bragg reflection planes of hexagonal wurtzite structure of ZnO corresponding to JCPDS Card No. 36-1451 [38-40]. As seen from XRD patterns of MIP/ZnO and NIP/ZnO nanocomposites, there is the same diffraction peak of

the hexagonal wurtzite structure of ZnO but with a lower intensity [41]. The FE-SEM and XRD results indicate the successful electropolymerization of MIP on ZnO NPs.

3.2. Electrochemical measurements

Figure 3 depicts the DPV curves of MIP/ZnO/CPE, NIP/ZnO/CPE, ZnO/CPE, and CPE at a scanning rate of 30 mV/s for a potential range of -0.90 to -0.10 V vs. Ag/AgCl in 0.1 M PBS of pH 4.0. The DPV curves are shown in both the absence and presence of cyanazine solutions in the electrochemical cell. In the absence of cyanazine solution, there is no clear peak in the DPV curves of the electrodes. After addition of the cyanazine solution, there are the anodic peaks at -0.39 V, -0.43 V, -0.56 V and -0.53 V at the DPV curves of MIP/ZnO/CPE, NIP/ZnO/CPE, ZnO/CPE and CPE, respectively, that can be related to the suggested electrochemical reduction process as shown in Figure 4 [21, 42, 43]. Figure 5 also shows that the DPV peak current of MIP/ZnO/CPE is greater than that of NIP/ZnO/CPE, ZnO/CPE, and CPE, and the cathodic peak appears at a significantly lower positive potential. It demonstrates a significant increase in MIP/ZnO/CPE electrocatalytic activity due to the synergistic effect of ZnO and MIPs. ZnO nanostructures with high electrocatalytic activity, large specific surface area [44], and high electrical conductivity can function as a highly porous surface to support MIP molecules in sensor design [45-47]. ZnO NPs also provide fast transfer of electrolyte ions to electrode through the electrochemical reactions and promote the sensitivity of the sensor [48-50].

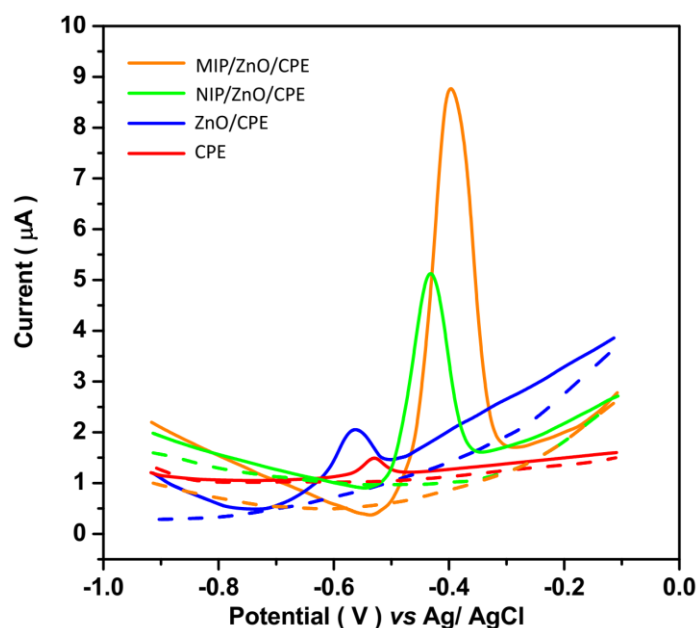


Figure 3. The DPV curves of MIP/ZnO/CPE, NIP/ZnO/CPE, ZnO/CPE and CPE at scanning rate of 30 mV/s for a potential range from -0.90 to -0.10 V vs. Ag/AgCl in 0.1 M PBS (pH 4.0) with (solid line) and without (dashed line) cyanazine solution.

In the case of MIP, the monomer(s) are first spontaneously arranged around the template to achieve a tailor-made cavity complementary to it during the electropolymerization process, whereas in NIP electropolymerization, there is no arrangement process due to the absence of the template molecules, resulting in a polymer with no imprinting (against the template molecule) and thus a less functional cavity [51, 52]. Thus, formation of 3D complementary cavities within the polymer during the synthesis and subsequently removal of the template molecule from the polymeric matrix results in cavities with specific shapes, structures and functional groups, which will serve as specific binding sites for the template [53]. Consequently, the MIP-based sensor shows improved sensitivity, selectivity and adsorption efficiency for the template [51]. Therefore, further electrochemical tests were conducted on MIP/ZnO/CPE.

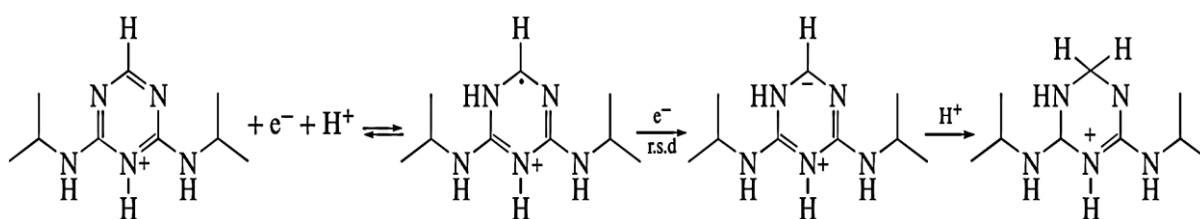


Figure 4. The suggested electrochemical reduction mechanism of cyanazine [21].

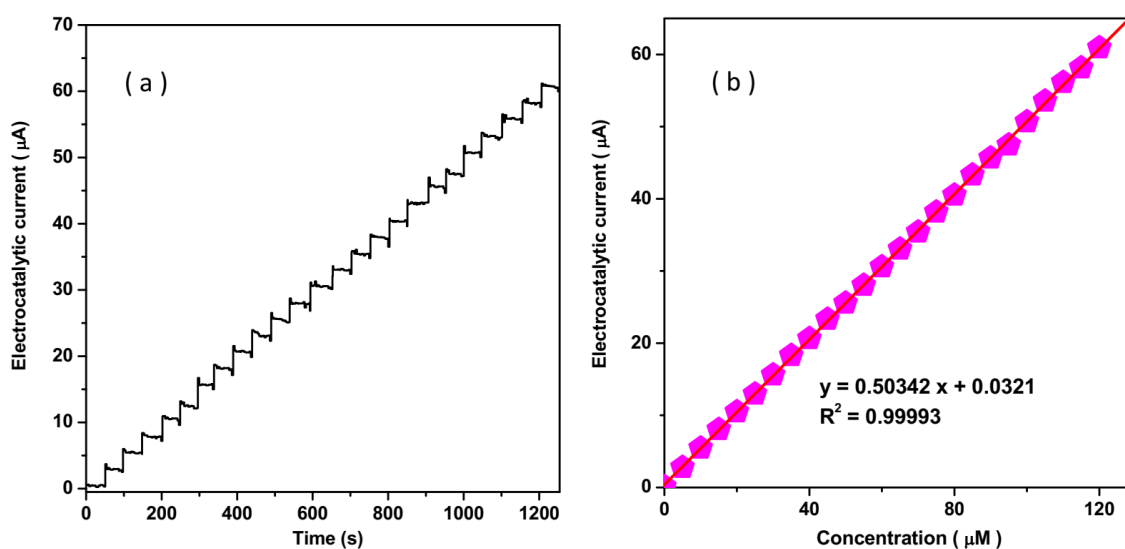


Figure 5. (a) The recorded amperogram of MIP/ZnO/CPE through successive injections of a solution containing 5 μM cyanazine in electrochemical cell containing 0.1 M PBS (pH 4.0) electrolyte solution at an applied potential of -0.39 V, and (b) the corresponding calibration graph.

Figure 5a depicts an amperogram of MIP/ZnO/CPE recorded after successive injections of a solution containing 5 μM cyanazine into an electrochemical cell containing 0.1 M PBS (pH 4.0)

electrolyte solution at an applied potential of -0.39 V. The recorded amperogram steps show a quick and sensitive response of the MIP/ZnO/CPE to each addition of cyanazine solution. By increasing the cyanazine concentration in the electrochemical cell, the amperometric current increases linearly, and the corresponding calibration graph in Figure 5b shows a linear response from 0 to 120 μM . The sensitivity of MIP/ZnO/CPE is determined to be 0.5034 $\mu\text{A}/\mu\text{M}$, and the limit of detection (LOD) is 5 nM.

Table 1 shows the comparison between the MIP/ZnO/CPE electrocatalytic performance and released outcomes of cyanazine sensors in literatures. In comparison to other reported cyanazine sensors, the proposed sensor in this study has a broad linear range for cyanazine concentrations and an appropriate LOD value. It can be attributed to grafting the MIP molecules as a special place for analyte detection on the porous surface of ZnO NPs with high conductivity and large surface area [54-56].

Table 1. Comparison between the MIP/ZnO/CPE electrocatalytic performance and released outcomes of cyanazine sensors in literatures.

Electrode	Technique	LOD (nM)	Linear range (μM)	Ref.
MIP/ZnO/CPE	Amperometry	5	0 to 120	Present work
GO/GCE	DPV	0.25	5.5×10^{-4} to 1.5	[21]
Pt-Pd-CdO/SWCNTs/ds-DNA/GCE	DPV	0.8	0.004 to 70	[57]
AuNP-CdTe quantum dots	fluorescent	0.156	5×10^{-5} to 9	[20]
Molecularly imprinted nanofilms onto the gold surfaces	surface plasmon resonance	0.095	10^{-4} to 6.64×10^{-3}	[18]
Monoclonal antibodies HYB/horseradish peroxidase	ELISA	4.15	1.6×10^{-6} to 6.23×10^{-3}	[16]
GLC columns	Gas Chromatography	0.78	0.00 to 2.36×10^{-3}	[17]
----	spectrophotometry	623.1	1.250 to 20.770	[15]
VP-ODS C18 column	HPLC	0.062	1.66×10^{-3} to 0.166	[19]

In agricultural wastewater samples, the specificity of the MIP/ZnO/CPE system was investigated in the presence of various chemicals and organic pesticides as interference species. Table 2 summarizes the results of amperometric measurements performed with MIP/ZnO/CPE after successive injections of a solution containing 100 nM cyanazine and 500 nM interference species solutions in 0.1M PBS (pH 4.0) at an applied potential of -0.39 V. The results show that when cyanazine solution is added to an electrochemical cell, a significant amperometric signal is formed. However, adding interference species to the electrolyte solution has no effect on the amperometric signal, demonstrating the high specificity of the MIP/ZnO/CPE to determine cyanazine in food in agricultural wastewater samples. This specificity is linked to tailor-made cavities in MIP as a special location for specific analytic detection [58].

Table 2. The results of amperometric measurements using MIP/ZnO/CPE upon successive injections of a solution containing 100 nM cyanazine and 500 nM interference species solutions in 0.1 M PBS (pH 4.0) at an applied potential of -0.39 V.

Substance	Added (nM)	Amperometric signal (μA) at -0.39 V	RSD
Cyanazine	100	0.0504	± 0.0020
Amylum	500	0.0078	± 0.0011
Glucose	500	0.0026	± 0.0012
Propazine	500	0.0109	± 0.0011
Carbofuran	500	0.0061	± 0.0010
Trichlorfon	500	0.0036	± 0.0007
Simetryn	500	0.0093	± 0.0011
Triazophos	500	0.0094	± 0.0008
Aminocarb	500	0.0070	± 0.0009
Isocarbophos	500	0.0061	± 0.0011
Phoxim	500	0.0074	± 0.0010
Dichlorvos	500	0.0090	± 0.0012
Isocarbophos	500	0.0076	± 0.0007
Diuron	500	0.0075	± 0.0007
Ca^{2+}	500	0.0051	± 0.0011
Na^+	500	0.0022	± 0.0010
Al^{3+}	500	0.0074	± 0.0011
Ag^+	500	0.0081	± 0.0012
Fe^{2+}	500	0.0084	± 0.0010
Mg^{2+}	500	0.0064	± 0.0010

The MIP/ZnO/CPE as a proposed sensing system for analysis of cyanazine in real samples prepared from lettuce samples was examined. Figure 6a shows the obtained data from amperometric measurements using MIP/ZnO/CPE upon successive injections of a solution containing 5 μM cyanazine in 0.1 M PBS (pH 4.0) prepared from a lettuce sample at an applied potential of -0.39 V. The resulted calibration graph in Figure 6b indicates that the cyanazine level in the processed sample is 5.20 μM , which is very close to the cyanazine concentration in the preparation of real sample process (5.19 μM). The analytical results are also summarized in Table 3, which illustrates that the values of RSD (3.48% to 4.64%) and recovery (99.20 to 99.60) are appropriate for valid and accurate practical analyses of food in agricultural wastewater samples.

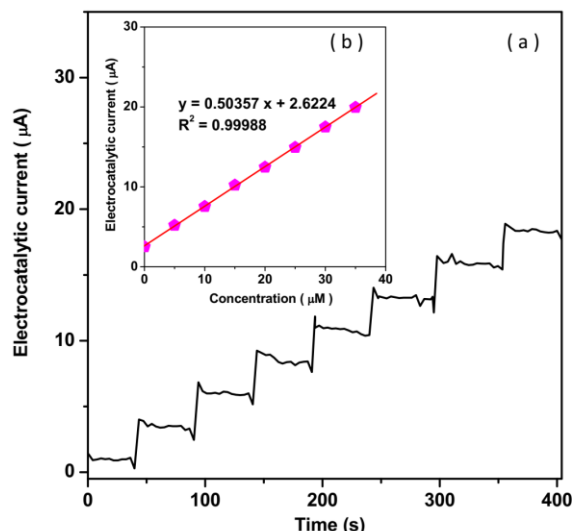


Figure 6. (a) The obtained data from amperometric measurements using MIP/ZnO/CPE upon successive injections of a solution containing 5 µM cyanazine in 0.1 M PBS (pH 4.0) prepared from lettuce sample at an applied potential of -0.39 V, and (b) the corresponding calibration graph.

Table 3. Analytical applicability of MIP/ZnO/CPE to determine cyanazine in real specimens.

Adding(µM)	Found(µM)	Recovery (%)	RSD (%)
5.00	4.96	99.20	3.48
10.00	9.94	99.40	3.66
15.00	14.90	99.33	4.58
20.00	19.92	99.60	4.64

4. CONCLUSION

The current work was done on the fabrication of MIP/ZnO/CPE for cyanazine determination in food samples. The ZnO NPs were electrodeposited on the CPE surface before the MIP layer was electropolymerized on the modified CPE. Structural studies of modified electrodes revealed the formation of ZnO NPs with a hexagonal shape characteristics and wurtzite-type structure on the CPE surface, and after electropolymerization, polymer nanoparticles were evenly dispersed on the nanostructured surface of ZnO, resulting in the formation of a rough-shaped nanocomposite. Because of the synergistic effect of ZnO and MIPs, electrochemical measurements revealed a significant increase in MIP/ZnO/CPE electrocatalytic activity and selectivity. The studies demonstrated a linear response from 0 to 120 µM, and the sensitivity of MIP/ZnO/CPE was determined to be 0.5034 µA/µM, with a LOD of 5nM. In comparison to other reported cyanazine sensors, the comparison of the MIP/ZnO/CPE electrocatalytic performance and released outcomes of cyanazine sensors in the literature revealed that the proposed sensor in this study presented a broad linear range of cyanazine

concentrations and an appropriate LOD value. The MIP/ZnO/CPE as a proposed sensing system for analysis of cyanazine in real samples prepared from lettuce samples was examined and the analytical results illustrated that the values of RSD and recovery were appropriate for valid and accurate practical analyses in food in agricultural wastewater samples.

ACKNOWLEDGEMENT

This work was sponsored in part by Key Scientific and technological projects of Jilin Province of China (2017020425N Y).

References

1. J. Dekker and S.O. Duke, *Advances in Agronomy*, 54 (1995) 69.
2. H. Karimi-Maleh, H. Beitollahi, P.S. Kumar, S. Tajik, P.M. Jahani, F. Karimi, C. Karaman, Y. Vasseghian, M. Baghayeri and J. Rouhi, *Food and Chemical Toxicology*, (2022) 112961.
3. X. Mo, X. Liu, J. Chen, S. Zhu, W. Xu, K. Tan, Q. Wang, Z. Lin and W. Liu, *Environmental Science: Nano*, 9 (2022) 1617.
4. Y. Zhang, C. Li, H. Ji, X. Yang, M. Yang, D. Jia, X. Zhang, R. Li and J. Wang, *International Journal of Machine Tools and Manufacture*, 122 (2017) 81.
5. C.B. Breckenridge, C. Werner, J.T. Stevens and D. Summer, *The triazine herbicides*, 50 (2008) 387.
6. X. Tang, J. Wu, W. Wu, Z. Zhang, W. Zhang, Q. Zhang, W. Zhang, X. Chen and P. Li, *Analytical chemistry*, 92 (2020) 3563.
7. R. Li, Z. Du, X. Qian, Y. Li, J.-C. Martinez-Camarillo, L. Jiang, M.S. Humayun, Z. Chen and Q. Zhou, *Quantitative Imaging in Medicine and Surgery*, 11 (2021) 918.
8. Y. Choi, J. Wang, Y. Zhu and W.-F. Lai, *Indian Journal of Pharmaceutical Education and Research*, 55 (2021) 63.
9. M. Yang, C. Li, Y. Zhang, D. Jia, X. Zhang, Y. Hou, R. Li and J. Wang, *International Journal of Machine Tools and Manufacture*, 122 (2017) 55.
10. W. Xu, C. LI, Y. Zhang, H.M. Ali, S. Sharma, R. Li, M. Yang, T. Gao, M. Liu and X. Wang, *International Journal of Extreme Manufacturing*, 4 (2022) 042003.
11. S. Schottler, S.J. Eisenreich and P. Capel, *Environmental science & technology*, 28 (1994) 1079.
12. H. Karimi-Maleh, C. Karaman, O. Karaman, F. Karimi, Y. Vasseghian, L. Fu, M. Baghayeri, J. Rouhi, P. Senthil Kumar and P.-L. Show, *Journal of Nanostructure in Chemistry*, 12 (2022) 429.
13. W.-F. Lai and W.-T. Wong, *Pharmaceutics*, 13 (2021) 787.
14. Z. Duan, C. Li, Y. Zhang, M. Yang, T. Gao, X. Liu, R. Li, Z. Said, S. Debnath and S. Sharma, *Frontiers of Mechanical Engineering*, (2022) 1.
15. G. Zhang and J. Pan, *Spectrochimica Acta Part A: Molecular and Biomolecular Spectroscopy*, 78 (2011) 238.
16. L. Bruun, C. Koch, M.H. Jakobsen and J. Aamand, *Food and agricultural immunology*, 12 (2000) 253.
17. D.C. Muir and B.E. Baker, *Journal of Agricultural and Food Chemistry*, 24 (1976) 122.
18. Y. Saylan, S. Akgönüllü, D. Çimen, A. Derazshamshir, N. Bereli, F. Yılmaz and A. Denizli, *Sensors and Actuators B: Chemical*, 241 (2017) 446.
19. Q. Zhou, Y. Ding and J. Xiao, *Chromatographia*, 65 (2007) 25.
20. L. Dong, C. Hou, M. Yang, H. Fa, H. Wu, C. Shen and D. Huo, *Journal of Nanoparticle Research*, 18 (2016) 164.
21. M.B. Gholivand, N. Karimian and M. Torkashvand, *Journal of Analytical Chemistry*, 70 (2015)

- 384.
22. W.-F. Lai, *Molecular pharmaceuticals*, 18 (2021) 1833.
 23. L. Tang, Y. Zhang, C. Li, Z. Zhou, X. Nie, Y. Chen, H. Cao, B. Liu, N. Zhang and Z. Said, *Chinese Journal of Mechanical Engineering*, 35 (2022) 1.
 24. A. Ghorbani, M.R. Ganjali, R. Ojani and J. Raoof, *International Journal of Electrochemical Science* 15 (2020) 2913.
 25. X. Wang, C. Li, Y. Zhang, Z. Said, S. Debnath, S. Sharma, M. Yang and T. Gao, *The International Journal of Advanced Manufacturing Technology*, 119 (2022) 631.
 26. H. Karimi-Maleh, R. Darabi, M. Shabani-Nooshabadi, M. Baghayeri, F. Karimi, J. Rouhi, M. Alizadeh, O. Karaman, Y. Vasseghian and C. Karaman, *Food and Chemical Toxicology*, 162 (2022) 112907.
 27. M. Ganjali, T. Alizade, B. Larijani, F. Faridbod and P. Norouzi, *International Journal of Electrochemical Science*, 7 (2012) 4756.
 28. X. Cui, C. Li, Y. Zhang, W. Ding, Q. An, B. Liu, H.N. Li, Z. Said, S. Sharma and R. Li, *Frontiers of Mechanical Engineering*, 18 (2023) 1.
 29. M.B. Gholivand and L. Mohammadi-Behzad, *Journal of Electroanalytical Chemistry*, 712 (2014) 33.
 30. L. Nan, C. Yalan, L. Jixiang, O. Dujuan, D. Wenhui, J. Rouhi and M. Mustapha, *RSC Advances*, 10 (2020) 27923.
 31. B. Patella, N. Moukri, G. Regalbuto, C. Cipollina, E. Pace, S. Di Vincenzo, G. Aiello, A. O’Riordan and R. Inguanta, *Materials*, 15 (2022) 713.
 32. K. Kor and K. Zarei, *Talanta*, 146 (2016) 181.
 33. S. Balayan, N. Chauhan, R. Chandra and U. Jain, *Biointerface Res. Appl. Chem*, 6 (2022) 38.
 34. Z. Zhang, F. Yang, H. Zhang, T. Zhang, H. Wang, Y. Xu and Q. Ma, *Materials Characterization*, 171 (2021) 110732.
 35. Q. Zhu, X. Li, Y. Xiao, Y. Xiong, S. Wang, C. Xu, J. Zhang and X. Wu, *Macromolecular Chemistry and Physics*, 218 (2017) 1700141.
 36. Y. Yang, Y. Gong, C. Li, X. Wen and J. Sun, *Journal of Materials Processing Technology*, 291 (2021) 117023.
 37. R. Li, X. Qian, C. Gong, J. Zhang, Y. Liu, B. Xu, M.S. Humayun and Q. Zhou, *IEEE Transactions on Biomedical Engineering*, (2022) 1.
 38. G. Krishna Reddy, A. Jagannatha Reddy, R. Hari Krishna, B. Nagabhushana and G.R. Gopal, *Journal of Asian Ceramic Societies*, 5 (2017) 350.
 39. M.-R. Wang, L. Deng, G.-C. Liu, L. Wen, J.-G. Wang, K.-B. Huang, H.-T. Tang and Y.-M. Pan, *Organic letters*, 21 (2019) 4929.
 40. C. Liu and J. Rouhi, *RSC Advances*, 11 (2021) 9933.
 41. J. Rouhi, H.K. Malayeri, S. Kakooei, R. Karimzadeh, S. Alrokayan, H. Khan and M.R. Mahmood, *International Journal of Electrochemical Science*, 13 (2018) 9742.
 42. H. Li, Y. Zhang, C. Li, Z. Zhou, X. Nie, Y. Chen, H. Cao, B. Liu, N. Zhang and Z. Said, *The International Journal of Advanced Manufacturing Technology*, 120 (2022) 1.
 43. S. Changaei, J. Zamir-Anvari, N.-S. Heydari, S.G. Zamharir, M. Arshadi, B. Bahrami, J. Rouhi and R. Karimzadeh, *Journal of Electronic Materials*, 48 (2019) 6216.
 44. Y. Zhao, Y. Moon and R. Savari, *International Journal of Electrochemical Science*, 17 (2022) 221185.
 45. A. Jana and D.H. Gregory, *Chemistry—A European Journal*, 26 (2020) 6703.
 46. H. Savaloni, E. Khani, R. Savari, F. Chahshouri and F. Placido, *Applied Physics A*, 127 (2021) 1.
 47. F. Chahshouri, H. Savaloni, E. Khani and R. Savari, *Journal of Micromechanics and Microengineering*, 30 (2020) 075001.
 48. M.L.M. Napi, S.M. Sultan, R. Ismail, K.W. How and M.K. Ahmad, *Materials*, 12 (2019) 2985.

49. Z. Savari, S. Soltanian, A. Noorbakhsh, A. Salimi, M. Najafi and P. Servati, *Sensors and Actuators B: Chemical*, 176 (2013) 335.
50. X. Cui, C. Li, Y. Zhang, Z. Said, S. Debnath, S. Sharma, H.M. Ali, M. Yang, T. Gao and R. Li, *Journal of Manufacturing Processes*, 80 (2022) 273.
51. A. Herrera-Chacón, X. Cetó and M. del Valle, *Analytical and Bioanalytical Chemistry*, 413 (2021) 6117.
52. Y. Yang, M. Yang, C. Li, R. Li, Z. Said, H.M. Ali and S. Sharma, *Frontiers of Mechanical Engineering*, (2022) 1.
53. A. Adumitrăchioaie, M. Tertiş, A. Cernat, R. Săndulescu and C. Cristea, *International Journal of Electrochemical Science*, 13 (2018) 2556.
54. C. Zhong, B. Yang, X. Jiang and J. Li, *Critical reviews in analytical chemistry*, 48 (2018) 15.
55. R. Savari, J. Rouhi, O. Fakhar, S. Kakooei, D. Pourzadeh, O. Jahanbakhsh and S. Shojaei, *Ceramics International*, 47 (2021) 31927.
56. X. Wang, C. Li, Y. Zhang, H.M. Ali, S. Sharma, R. Li, M. Yang, Z. Said and X. Liu, *Tribology International*, 174 (2022) 107766.
57. H. Karimi-Maleh, F. Karimi, L. Fu, A.L. Sanati, M. Alizadeh, C. Karaman and Y. Orooji, *Journal of Hazardous Materials*, 423 (2022) 127058.
58. Y. Ma, S. Xu, S. Wang and L. Wang, *TrAC Trends in Analytical Chemistry*, 67 (2015) 209.

© 2022 The Authors. Published by ESG (www.electrochemsci.org). This article is an open access article distributed under the terms and conditions of the Creative Commons Attribution license (<http://creativecommons.org/licenses/by/4.0/>).